RSC Advances

PAPER

View Article Online
View Journal | View Issue

Cite this: *RSC Adv.*, 2022, **12**, 874

A dual responsive fluorescent probe for selective detection of cysteine and bisulfite and its application in bioimaging†

Xiaofeng Wang,‡[a] Mingshun Li,‡[b] Tingting Duan,*[a] Yuxia Zou*[a] and Xuejun Zhou *[a]

A coumarin-based dual responsive fluorescent probe with a simple structure was developed for the detection of Cys and HSO_3^-. Under simulated physiological conditions, Cou-F displayed an on–off fluorescence response to Cys at 521 nm and an off–on fluorescence response to HSO_3^- at 500 nm. Furthermore, Cou-F had the advantages of high sensitivity, strong specificity and rapid response. The detection limits of Cou-F toward Cys and HSO_3^- were 0.54 μM and 0.65 μM, respectively. Cou-F enabled high selective responses to Cys and HSO_3^- over other biologically related species. The response times of Cou-F toward Cys and HSO_3^- were 80 s and 100 s. The fluorescence imaging of Cys and HSO_3^- was achieved in living RAW246.7 cells.

Received 12th November 2021
Accepted 17th December 2021

DOI: 10.1039/d1ra08317a

rsc.li/rsc-advances

Introduction

Cysteine (Cys), a small molecule amino acid containing a sulfhydryl group, plays critical roles in maintaining the redox homeostasis of organisms.[1–3] It has been found that Cys is involved in many physiological and pathological processes.[4] Abnormal fluctuations in Cys levels are directly associated with many diseases, such as liver damage, lethargy, and cardiovascular disease.[5–7] As an important preservative for many foods, beverages and pharmaceuticals, bisulfite (HSO_3^-) not only can be used as an antioxidant to inhibit bacterial growth, but also control enzymatic reactions during production and storage. It has been confirmed that certain concentration levels can cause asthma and anaphylactic reaction.[8,9] In addition, HSO_3^- has a toxic effect on cells, tissues and organisms. It can cause irreversible damage, such as cell necrosis, inhibit cell mitosis, induce chromosomal aberrations and ultimately lead to cell death.[10–12] Although significant progress has been achieved in the biological chemistry of Cys and HSO_3^-, the physiological functions of Cys and HSO_3^- still need to be further uncovered.

Traditional methods for detecting Cys and HSO_3^- including high-performance liquid chromatography, colorimetry, electrochemical analysis and capillary electrophoresis have been widely used.[13,14] However, these detection methods require cumbersome sample preparation, time-consuming detection processes, expensive operating costs and cannot be directly detected *in vivo*. As an advanced detection tool, fluorescent probes can perform selective and highly sensitive detection of biologically active species in organisms.[15–17] Most importantly, fluorescent probes enter cells and tissues in a non-invasive manner without destroying their integrity. Considering the importance of Cys and HSO_3^- in organisms, the development of sensitive and selective fluorescent probes for Cys and HSO_3^- are greatly useful. So far, various reactions have been explored to design Cys fluorescent probes such as nucleophilic substitution reaction, Michael addition reaction, sulfonate or sulfonamide cleavage reaction and so on.[18–26] The design of HSO_3^- fluorescent probes is mainly based on nucleophilic addition reaction of unsaturated double bonds including –C=O bonds, –C=C bonds, –N=N bonds and –C=N bonds.[27–37] Although fluorescent probes for Cys and HSO_3^- have obtained a development, the use of a single fluorophore to distinguish Cys and HSO_3^- at different emission channels still faces challenges.

In this work, we report a dual responsive fluorescent probe Cou-F for Cys and HSO_3^-. Cou-F displays selective and sensitive detection of Cys and HSO_3^- at different fluorescence emission modes. Significantly, Cou-F can be successfully employed for imaging Cys and HSO_3^- in living cells, which suggested its great potential for exploring the physiological and pathological processes related to Cys and HSO_3^-.

Results and discussion

Probe design

To develop an ideal fluorescent probe for the detection of Cys and HSO_3^-, choosing a suitable fluorophore was essential for its successful application in complex biological environments. The

[a]*Department of Otolaryngology, Head and Neck Surgery, The First Affiliated Hospital of Hainan Medical University, Haikou 570102, China. E-mail: xuejunzhouent@hainmc.edu.cn; denieceduan@163.com; zouyuxiazzz@163.com*

[b]*School of Pharmaceutical Sciences, Southern Medical University, Guangzhou, 510515, China*

† Electronic supplementary information (ESI) available. See DOI: 10.1039/d1ra08317a

‡ These authors contributed equally.

coumarin derivative was one of the best choices due to its excellent pharmacokinetics and good biocompatibility. Cou-F had a typical push–pull electronic structure. The detailed synthesis route and NMR, HRMS spectrum data of Cou-F were shown in ESI (Fig. S1–S6†). In this design, an aldehyde was not only an electron-withdrawing group but also a reactive site (Scheme 1). In the presence of Cys, the aldehyde of Cou-F could react specifically with Cys to give thiazolidine which led to a decrease in fluorescence intensity. This decrease in fluorescence might be caused by the photo-induced electron transfer mechanism triggered by adjacent nitrogen atoms on the thiazolidine ring. As we all know, the selective reaction of aldehyde and HSO_3^- is a classic nucleophilic-addition reaction in organic chemistry. Based on this reaction, we found that the aldehyde of Cou-F also reacted with HSO_3^- to generate an adduct Cou-F–HSO_3^- and touch off fluorescence enhancement. The possible reaction mechanism was verified by HRMS (Fig. S7 and S8†). The reaction of Cou-F and Cys or HSO_3^- were performed in the mixture solution system (DMSO/H_2O = 1/1, v/v). The HRMS assay of the reaction product of Cou-F and Cys displayed two peaks at *m*/*z* 270.1125 and 372.1146, which were attributed to Cou-F and Cou-F–Cys. Two prominent peaks at *m*/*z* 270.1126 and 374.0665 corresponding to Cou-F and Cou-F–HSO_3^- were observed.

Spectroscopic evaluation of Cou-F

We first investigated the spectroscopic properties of Cou-F toward Cys and HSO_3^- under simulated physiological conditions (10 mM HEPES, pH 7.4). Upon excitation at 450 nm or 432 nm, Cou-F emitted moderate-intensity fluorescence (Fig. 1A and B). As anticipated, upon the addition of Cys to the Cou-F solution, the fluorescence intensity at 521 nm of Cou-F decreased sharply with the increase of Cys concentration (λ_{ex} = 450 nm, Fig. 1A). As depicted in Fig. 1B, the addition of HSO_3^- resulted in a significant increase in fluorescence intensity at 500 nm under the excitation at 432 nm (up to 5-fold). Cou-F showed excellent linear responses to Cys and HSO_3^- within 0–100 μM. The detection limits ($3\sigma/k$) of Cys and HSO_3^- were calculated to be 0.54 μM and 0.65 μM, respectively (Fig. 1C and D). The photostability of probe Cou-F was a crucial factor in exploring live cells and *in vivo* imaging. The fluorescence intensity of Cou-F could be maintained stale within 100 min, which suggested Cou-F had good photostability and could be applied for biological imaging (Fig. 1E and F).

Next, we tested the reaction kinetics of Cou-F. As shown in Fig. 2A, when 100 μM of Cys was added, the fluorescence intensity of Cou-F at 521 nm decreased and reached a plateau during 80 s. Upon the addition of 100 μM of HSO_3^-, the

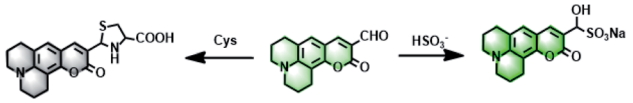

Scheme 1 The chemical structure of Cou-F and its proposed response mechanism towards Cys and HSO_3^-.

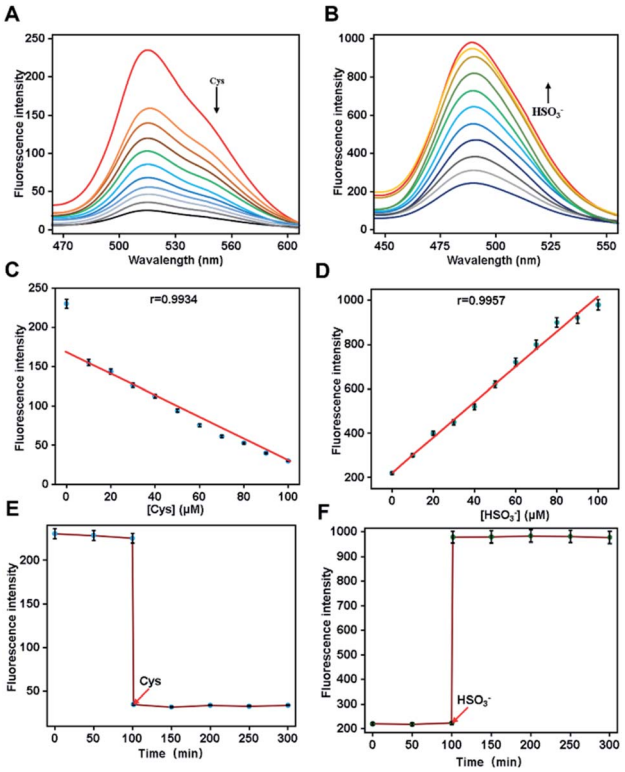

Fig. 1 (A) Fluorescence spectra of Cou-F (10 μM) with the increasing concentrations of Cys (0–100 μM). λ_{ex} = 450 nm. (B) Fluorescence spectra of Cou-F (10 μM) with the increasing concentrations of HSO_3^- (0–100 μM). λ_{ex} = 432 nm. (C) Linear relationship between fluorescence intensities at 521 nm with concentrations of Cys. (D) Linear relationship between fluorescence intensities at 500 nm with concentrations of HSO_3^-. (E) The photostability of Cou-F and Cou-F–Cys. (F) The photostability of Cou-F and Cou-F–HSO_3^-.

fluorescence intensity of Cou-F increased and reached balance in 100 s (Fig. 2B). The results demonstrated that Cou-F enabled rapid detection of Cys and HSO_3^-.

The influence of different pH values on the fluorescence response properties of Cou-F was also examined. The fluorescence intensity of Cou-F and Cou-F–Cys had barely changed in the pH range from 2.0 to 9.0, indicating that Cou-F and Cou-F–Cy were not pH sensitive (Fig. 2C). In addition, Cou-F showed off–on fluorescence responses toward HSO_3^- over a wide pH range of 4.0–9.0 (Fig. 2D). The results evidenced Cou-F was a useful tool for the detection of Cys and HSO_3^- under physiological conditions. Excellent selectivity was an essential feature of an ideal probe, which directly determined the application of the probe in complex biological systems. Various biologically related species such as amino acids (Ala, Asn, Arg, Asp, Gln, Glu, Gly, His, Ile, Leu, Lys, Met, GSH, Hcy, Pro, Ser, Thr, Trp, Tyr, Val), reactive oxygen species (HClO, H_2O_2), reactive nitrogen species (NO), anion (HS^-, Cl^-, SO_4^{2-}, $H_2PO_4^-$, SCN^-, $S_2O_3^{2-}$) were selected for the evaluation of the probe Cou-F selectivity. Except for the slight decrease in fluorescence intensity caused by Hcy, other species hardly induced fluorescence change (Fig. S9†). As demonstrated in Fig. S10,† common interfering species in living systems caused no change to the fluorescence

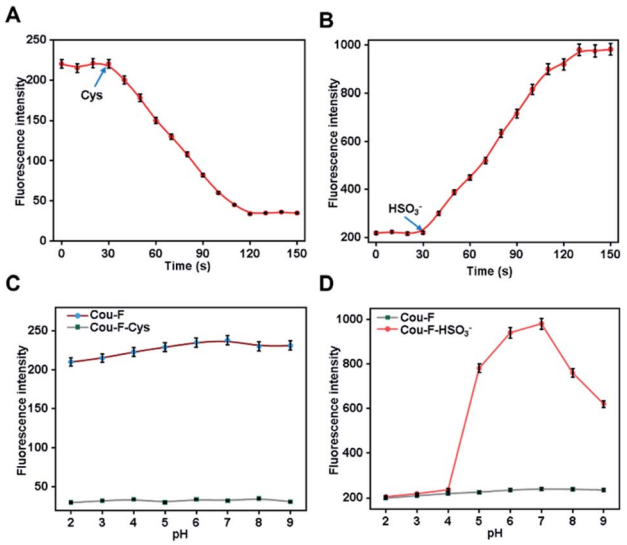

Fig. 2 (A) The reaction kinetics of Cou-F (10 μM) with Cys (100 μM). (B) The reaction kinetics of Cou-F (10 μM) with HSO_3^- (100 μM). (C) pH-dependent fluorescence intensities at 521 nm of Cou-F (10 μM) in the absence or presence of Cys (100 μM). (D) pH-dependent fluorescence intensities at 500 nm of Cou-F (10 μM) in the absence or presence of HSO_3^- (100 μM).

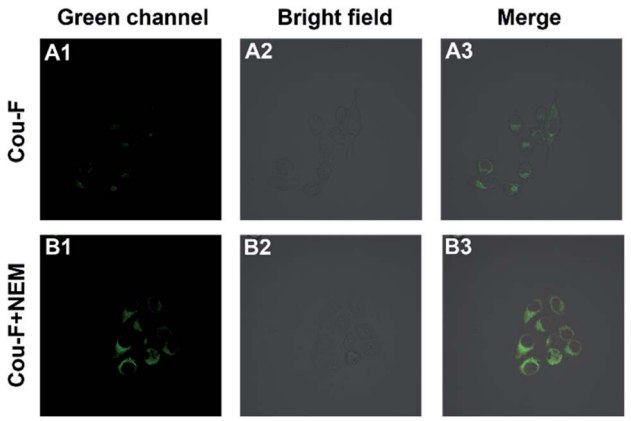

Fig. 3 Confocal images of Cys in RAW246.7 cells. (A) The cells incubated with Cou-F (10 μM) for 30 min. (B) The cells pre-treated with 1 mM NEM for 30 min, then stained with Cou-F (10 μM) for 30 min. Green channel: λ_{em} = 510–530 nm (λ_{ex} = 488 nm).

intensity of Cou-F except for HSO_3^-. Taken together, Cou-F showed good selectivity and was suitable for bioimaging.

Cell imaging

Considering the outstanding properties of Cou-F, we set out to explore its potential application in cell imaging. Confocal laser microscope was applied for the imaging experiment of Cou-F in RAW246.7 cells. Before imaging, we used CCK-8 to evaluate the cytotoxicity of Cou-F. As shown in Fig. S6,† the cell viability remained above 80% even if 100 μM of Cou-F was added (Fig. S11†). The results confirmed that Cou-F had low cytotoxicity and good biocompatibility. Subsequently, fluorescence

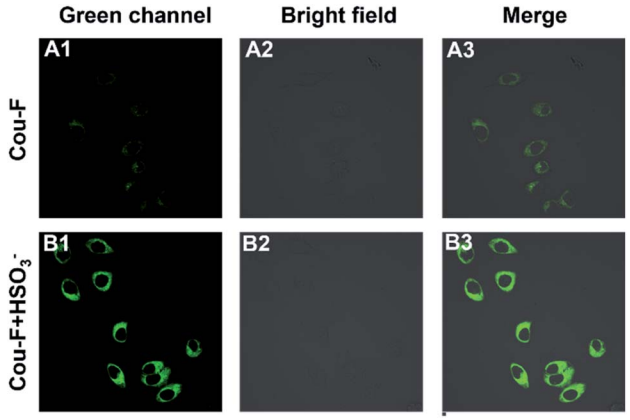

Fig. 4 Confocal images of HSO_3^- in RAW246.7 cells. (A) The cells pre-treated with 1 mM NEM for 30 min, then stained with Cou-F (10 μM) for 30 min. (B) The cells pre-treated with 1 mM NEM for 30 min, then stained with Cou-F (10 μM) for 30 min, and further treated with HSO_3^- (100 μM) for 30 min. Green channel: λ_{em} = 490–505 nm (λ_{ex} = 488 nm).

imaging of endogenous Cys in living RAW246.7 cells using Cou-F was performed. The RAW246.7 cell line was divided into two groups. In the first group, the cells were cultured with 10 μM Cou-F at 37 °C for 30 min, and then washed with phosphate buffer saline three times. As depicted in Fig. 3, weak green fluorescence was observed. In the second group, the cells pre-treated with 1 mM *N*-ethylmaleimide (a widely used thiol scavenger) and co-incubated with 10 μM Cou-F emitted moderate green fluorescence. We also further explored the application of Cou-F to imaging of HSO_3^- in living cells (Fig. 4). The cells that were pre-treated with 1 mM NEM, then stained with 10 μM Cou-F displayed moderate green fluorescence. Upon the addition of 100 μM HSO_3^- to the cells, an increased green fluorescence was observed. The images demonstrated that Cou-F not only showed satisfactory cell membrane penetration but also could detect Cys and HSO_3^- at the cell level.

Conclusions

In summary, we designed and synthesized a coumarin-based dual responsive fluorescent probe Cou-F for sensing of Cys and HSO_3^-. Cou-F was highly sensitive and selective for the detection of Cys and HSO_3^-. With the treatment of Cys, the fluorescence of Cys decreased at 521 nm, while upon the addition of HSO_3^-, the turn-on fluorescence responses at 500 nm were seen. Moreover, Cou-F featured low cytotoxicity and excellent cell permeability and was successfully used for imaging of Cys and HSO_3^- in living RAW246.7 cells. As a powerful chemical tool, the probe Cou-F has great potential in the imaging study of Cys and HSO_3^- in cells.

Author contributions

The manuscript was written through contributions of all authors. All authors have given approval to the final version of the manuscript.

Conflicts of interest

There are no conflicts to declare.

Acknowledgements

This work was supported by the Natural Science Foundation of Hainan Province (820MS141, 819MS121).

Notes and references

1 K. Ulrich and U. Jakob, *Free Radical Biol. Med.*, 2019, **140**, 14–27.
2 G. J. McBean, M. Aslan, H. R. Griffiths and R. C. Torrão, *Redox Biol.*, 2015, **5**, 186–194.
3 N. J. Pace and E. Weerapana, *ACS Chem. Biol.*, 2013, **8**, 283–296.
4 D. W. Bak and E. Weerapana, *Mol. BioSyst.*, 2015, **11**, 678–697.
5 A. Pastore, A. Alisi, G. di Giovamberardino, A. Crudele, S. Ceccarelli, N. Panera, C. Dionisi-Vici and V. Nobili, *Int. J. Mol. Sci.*, 2014, **15**, 21202–21214.
6 M. op den Winkel, L. Gmelin, J. Schewe, N. Leistner, M. Bilzer, B. Göke, A. L. Gerbes and C. J. Steib, *Lab. Invest.*, 2013, **93**, 1288–1294.
7 L. El-Khairy, P. M. Ueland, H. Refsum, I. M. Graham and S. E. Vollset, *Circulation*, 2001, **103**, 2544–2549.
8 T. Fazio and C. R. Warner, *Food Addit. Contam.*, 1990, **7**, 433–454.
9 R. F. McFeeters, *J. Food Prot.*, 1998, **61**, 885–890.
10 Z. Meng, *Inhalation Toxicol.*, 2003, **15**, 181–195.
11 Z. Meng and B. Zhang, *Environ. Toxicol. Pharmacol.*, 2003, **13**, 1–8.
12 Y. Zhai, X. L. Huang, H. J. Ma, X. H. Zhou, J. L. Zhou and Y. M. Fan, *Cent. Eur. J. Immunol.*, 2019, **44**, 226–236.
13 A. M. Pisoschi, A. Pop, I. Gajaila, F. Iordache, R. Dobre, I. Cazimir and A. I. Serban, *Microchem. J.*, 2020, **155**, 104681.
14 J. Huang, W. Qu, J. Zhu, H. Liu, W. Wen, X. Zhang and S. Wang, *Sens. Actuators, B*, 2019, **284**, 451–455.
15 K. Li, S. Xu, M. Xiong, S. Y. Huan, L. Yuan and X. B. Zhang, *Chem. Soc. Rev.*, 2021, DOI: 10.1039/D1CS00408E.
16 H. Liu, M. N. Radford, C. T. Yang, W. Chen and M. Xian, *Br. J. Pharmacol.*, 2019, **176**, 616–627.
17 D. Cao, Z. Liu, P. Verwilst, S. Koo, P. Jangjili, J. S. Kim and W. Lin, *Chem. Rev.*, 2019, **119**, 10403–10519.
18 X. Yue, J. Chen, W. Chen, B. Wang, H. Zhang and X. Song, *Spectrochim. Acta, Part A*, 2021, **250**, 119347.
19 T. C. Pham, Y. Choi, C. Bae, C. S. Tran, D. Kim, O.-S. Jung, Y. C. Kang, S. Seo, H. S. Kim, H. Yun, X. Zhou and S. Lee, *RSC Adv.*, 2021, **11**, 10154–10158.
20 W. Y. O, W. C. Chan, C. Xu, J. R. Deng, B. C. B. Ko and M. K. Wong, *RSC Adv.*, 2021, **11**, 33294–33299.
21 W. Luo, S. Zhang, Q. Meng, J. Zhou, R. Jin, X. Long, Y.-P. Tang and H. Guo, *Talanta*, 2021, **224**, 121833.
22 S. Han, H. Zhang, X. Yue, J. Wang, L. Yang, B. Wang and X. Song, *Anal. Chem.*, 2021, **93**, 10934–10939.
23 L. Zhao, X. He, Y. Huang, S. Zhang, H. Han, L. Xu, X. Wang, D. Song, P. Ma and Y. Sun, *Anal. Bioanal. Chem.*, 2020, **412**, 7211–7217.
24 B. Feng, Y. Liu, S. Huang, X. Huang, L. Huang, M. Liu, J. Wu, T. Du, S. Wang, X. Feng and W. Zeng, *Sens. Actuators, B*, 2020, **325**, 128786.
25 S. Cai, C. Liu, X. Jiao, L. Zhao and X. Zeng, *J. Mater. Chem. B*, 2020, **8**, 2269–2274.
26 F. Z. Chen, Z. Chen, Y. C. Sun, H. Liu, D. M. Han, H. P. He, X. H. Zhang and S. F. Wang, *RSC Adv.*, 2017, **7**, 16387–16391.
27 L. Xie, R. Zheng, H. Hu and L. Li, *Microchem. J.*, 2022, **172**, 106931.
28 J. S. Lan, R. F. Zeng, Y. Wang, L. Zhen, Y. Liu, R. J. Y. Ho, Y. Ding and T. Zhang, *J. Hazard. Mater.*, 2022, **424**, 127229.
29 Y. Wang, F. Zhou, Q. Meng, S. Zhang, H. Jia, C. Wang, R. Zhang and Z. Zhang, *Chem.–Asian J.*, 2021, **16**, 3419–3426.
30 L. Wang, L. Zhao, Z. Xu, Y. Ma, X. Wang, Q. Sun and H. Liu, *Microchem. J.*, 2021, **160**, 105703.
31 Z. Peng, L. Shi, X. Zeng, S. Yang, J. Xiao, S. Gong, H. Xiang and G. Shao, *Dyes Pigm.*, 2021, **186**, 108972.
32 H. Feng, J. Liu, A. Qaitoon, Q. Meng, Y. Sultanbawa, Z. Zhang, Z. P. Xu and R. Zhang, *TrAC, Trends Anal. Chem.*, 2021, **136**, 116199.
33 R. Zhou, G. Cui, Y. Hu, Q. Qi, W. Huang and L. Yang, *RSC Adv.*, 2020, **10**, 25352–25357.
34 K. Zhong, L. Chen, X. Yan, Y. Tang, S. Hou, X. Li and L. Tang, *Dyes Pigm.*, 2020, **182**, 108656.
35 Q. Jiang, Z. Wang, M. Li, J. Song, Y. Yang, X. Xu, H. Xu and S. Wang, *Tetrahedron Lett.*, 2020, **61**, 152103.
36 Z. Deng, F. Li, G. Zhao, W. Yang and Y. Hu, *RSC Adv.*, 2020, **10**, 26349–26357.
37 Z. Chen, F. Z. Chen, Y. C. Sun, H. Liu, H. P. He, X. H. Zhang and S. F. Wang, *RSC Adv.*, 2017, **7**, 2573–2577.